Novel Strategy for a Cocktail ^{18}F-Fluoride and ^{18}F-FDG PET/CT Scan for Evaluation of Malignancy: Results of the Pilot-Phase Study

Andrei Iagaru[1], Erik Mittra[1], Shahriar S. Yaghoubi[2], David W. Dick[2], Andrew Quon[1], Michael L. Goris[1], and Sanjiv Sam Gambhir[1,3]

[1]Division of Nuclear Medicine, Stanford University Medical Center, Stanford, California; [2]Molecular Imaging Program at Stanford (MIPS), Stanford University, Stanford, California; and [3]Departments of Radiology and Bioengineering, Molecular Imaging Program at Stanford (MIPS), Stanford University Medical Center, Stanford, California

^{18}F-FDG PET/CT is used for detecting cancer and monitoring cancer response to therapy. However, because of the variable rates of glucose metabolism, not all cancers are identified reliably. Sodium ^{18}F was previously used for bone imaging and can be used as a PET/CT skeletal tracer. The combined administration of ^{18}F and ^{18}F-FDG in a single PET/CT study for cancer detection has not been reported to date. **Methods:** This is a prospective pilot study (November 2007–November 2008) of 14 patients with proven malignancy (6 sarcoma, 3 prostate cancer, 2 breast cancer, 1 colon cancer, 1 lung cancer, and 1 malignant paraganglioma) who underwent separate ^{18}F PET/CT and ^{18}F-FDG PET/CT and combined ^{18}F/^{18}F-FDG PET/CT scans for the evaluation of malignancy (a total of 3 scans each). There were 11 men and 3 women (age range, 19–75 y; average, 50.4 y). **Results:** Interpretation of the combined ^{18}F/^{18}F-FDG PET/CT scans compared favorably with that of the ^{18}F-FDG PET/CT (no lesions missed) and the ^{18}F PET/CT scans (only 1 skull lesion seen on an ^{18}F PET/CT scan was missed on the corresponding combined scan). Through image processing, the combined ^{18}F/^{18}F-FDG scan yielded results for bone radiotracer uptake comparable to those of the ^{18}F PET/CT scan performed separately. **Conclusion:** Our pilot-phase prospective trial demonstrates that the combined ^{18}F/^{18}F-FDG administration followed by a single PET/CT scan is feasible for cancer detection. This combined method opens the possibility for improved patient care and reduction in health care costs.

Key Words: ^{18}F; ^{18}F-FDG; PET/CT; malignancy

J Nucl Med 2009; 50:501–505
DOI: 10.2967/jnumed.108.058339

The role of ^{18}F-FDG PET/CT is proven in a variety of cancers, including lymphoma, colorectal carcinoma, lung cancer, and melanoma, entities for which ^{18}F-FDG PET/CT has changed the practice of oncology (*1*). However, because of the variable rates of glucose metabolism, not all malignant lesions are identified reliably, contributing to the overall limitations of ^{18}F-FDG PET/CT (*2*).

Initial staging of patients diagnosed with certain cancers involves imaging with ^{18}F-FDG PET/CT and ^{99m}Tc-methylenediphosphonate (^{99m}Tc-MDP) bone scintigraphy (*3,4*). Bone scintigraphy with sodium ^{18}F was performed before the introduction of ^{99m}Tc-based agents, achieving excellent quality studies (*5*). ^{18}F is a positron emitter, allowing for PET. Thus, imaging skeletal lesions with ^{18}F PET/CT appears a logical approach for acquisition of highly sensitive and specific images.

Combining ^{18}F and ^{18}F-FDG in a single PET/CT scan for cancer detection has not been reported to date. However, if successful, such an approach has the potential to improve cancer diagnosis, staging, and possibly therapy monitoring. Therefore, we were prompted to prospectively evaluate the feasibility of the combined administration of ^{18}F and ^{18}F-FDG in a single PET/CT examination for pretherapy evaluation of extent of disease in patients with cancer.

MATERIALS AND METHODS

Preclinical Study

Approval was obtained from the Stanford University Administrative Panel on Laboratory Animal Care. Four mice were imaged with small-animal PET 1 h after tail vein administration of ^{18}F (7,400 kBq [200 μCi]), ^{18}F-FDG (7,400 kBq [200 μCi]), and combined ^{18}F/^{18}F-FDG (3,700 kBq [100 μCi] of each radiopharmaceutical) on separate days. Immediately after the combined ^{18}F/^{18}F-FDG PET, a micro-CT scan was obtained. Fiducial markers were placed for coregistration of the small-animal PET and micro-CT images. PET images were acquired using a microPET rodent R4 scanner (Concorde Microsystems). CT images were obtained using an eXplore RS MicroCT system (GE Healthcare). The CT data were used to create a bone mask that allowed the display of ^{18}F/^{18}F-FDG in the osseous structures on the PET scan. The image processing involved in this preclinical study required obtaining a bone mask from CT data, combining ^{18}F/^{18}F-FDG PET data with micro-CT data for coregistration (using fiducial markers), and displaying the ^{18}F/^{18}F-FDG uptake in the osseous structures on the PET scan. The processed images were

Received Sep. 21, 2008; revision accepted Dec. 24, 2008.
For correspondence or reprints contact: Sanjiv S. Gambhir, James H. Clark Center, 318 Campus Dr., 150 E. Wing, 1st Floor, Stanford, CA 94305–5427.
E-mail: sgambhir@stanford.edu

compared with those obtained after separate ^{18}F PET and ^{18}F-FDG PET scans (Supplemental Fig. 1; supplemental materials are available online only at http://jnm.snmjournals.org).

Clinical Study

The clinical component was approved by the Stanford University Institutional Review Board and the Cancer Center Scientific Committee. A total of 14 consecutive patients (3 women and 11 men; mean age ± SD, 50.4 ± 17.8 y, age range, 19–75 y) were recruited for this pilot-phase study. Their diagnoses were soft-tissue sarcoma (4 patients), prostate cancer (3 patients), breast cancer (2 patients), osteosarcoma (2 patients), colon cancer (1 patient), lung cancer (1 patient), and malignant paraganglioma (1 patient). The patients underwent a separate ^{18}F PET/CT scan and a separate ^{18}F-FDG PET/CT scan, followed by a combined administration of ^{18}F/^{18}F-FDG for the third PET/CT scan. All 3 scans were obtained within a 2-wk interval.

PET/CT Protocols and Image Reconstruction

Whole-body PET/CT images were obtained in 2D mode using a GE Discovery LT scanner (GE Healthcare). The PET images were reconstructed with a standard iterative algorithm (ordered-subset expectation maximization, 2 iterative steps, 28 subsets). Images were reformatted into axial, coronal, and sagittal views and reviewed with the software provided by the manufacturer (Xeleris, version 2.0551; GE Medical Systems, Haifa, Israel). The prescribed radiotracer doses were 555 MBq (15 mCi) for ^{18}F-FDG, 370 MBq (10 mCi) for ^{18}F, and 555 MBq (15 mCi) of ^{18}F-FDG + 185 MBq (5 mCi) of ^{18}F for the combined (cocktail) scan. For the combined ^{18}F/^{18}F-FDG scans, the 2 radiotracers were delivered from the local cyclotron facility in separate syringes and administered sequentially, without delay between the 2. PET and CT images were obtained starting at 60 min after intravenous administration of the radiotracers.

Image Analysis

The ^{18}F PET/CT, ^{18}F-FDG PET/CT, and combined ^{18}F/^{18}F-FDG PET/CT scans were interpreted by 2 board-certified nuclear medicine readers unaware of the diagnosis and results of the other imaging studies. In addition to the separate interpretation of the 3 scans for each patient, the CT data from the combined ^{18}F/^{18}F-FDG scan were used to create a bone mask that allowed the display of ^{18}F/^{18}F-FDG in the osseous structures on the PET scan. The first step was to reformat the CT to the dimensions of the PET scan (i.e., $128^2 \times n$ from $512^2 \times n$). The CT was interactively thresholded to eliminate all soft tissue but keep the bone densities. The nonzero values are made 1 to form a digital bone mask. The PET image multiplied by the mask left the bone image with a combined ^{18}F/^{18}F-FDG signal. These steps are illustrated in Figure 1. Each detected lesion was directly compared among the 3 PET/CT scans.

RESULTS

Evaluation of Combined ^{18}F/^{18}F-FDG PET of Mice

We first investigated the feasibility of combined ^{18}F/^{18}F-FDG PET in mice. Through the aid of a bone mask from the micro-CT and using the fiducial markers for coregistration of CT and PET images, we processed the small-animal PET images of mice obtained after administration of combined ^{18}F/^{18}F-FDG to display only the combined radiotracer uptake in the skeleton. These images compared favorably with the images obtained from the ^{18}F PET scan alone, supporting the translation of this method to a pilot clinical trial.

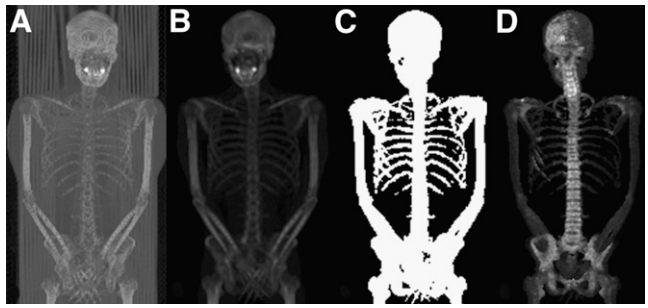

FIGURE 1. (A) The first step is to reformat CT image to dimensions of PET image. (B) Bed is eliminated by indicating most dependent part of body as image limit. (C) CT image is interactively thresholded to eliminate all soft tissue but keep bone densities. (D) PET image multiplied by mask leaves bone image with combined ^{18}F/^{18}F-FDG uptake.

Evaluation of Combined ^{18}F/^{18}F-FDG PET/CT Versus ^{18}F PET/CT in Humans

We then investigated bone images acquired with combined ^{18}F/^{18}F-FDG PET/CT versus ^{18}F PET/CT performed separately. For this comparison, we used the image-processing algorithm validated by the mouse study and visual analysis of the ^{18}F/^{18}F-FDG PET/CT scans.

Through image processing, the combined ^{18}F/^{18}F-FDG scan yielded results for bone radiotracer uptake comparable to those of the ^{18}F PET/CT scan performed separately. Thus, the combined ^{18}F/^{18}F-FDG cocktail tracer administration followed by single PET/CT appears to be feasible in this patient population referred for pretherapy evaluation of the extent of a known malignancy.

Visual analysis of the combined ^{18}F/^{18}F-FDG PET/CT scans without processing compared favorably with that of the ^{18}F PET/CT scans. The results of this analysis are presented in Table 1. There was no disagreement (in this limited number of scans) between the readers. Only 1 skull lesion seen on an ^{18}F scan was missed on the corresponding combined scan; however, this did not change the patient's management because other skeletal lesions were identified. Figure 2 shows a 44-y-old man with soft-tissue sarcoma (patient 6). Both ^{18}F and combined ^{18}F/^{18}F-FDG scans can show more extensive skeletal disease, as does the case presented in Figure 3 (patient 4).

Evaluation of Combined ^{18}F/^{18}F-FDG PET/CT Versus ^{18}F-FDG PET/CT in Humans

For all the patients enrolled, visual analysis of the combined ^{18}F/^{18}F-FDG PET/CT scans shows that ^{18}F/^{18}F-FDG images allow for accurate interpretation of the radiotracer uptake in the soft tissues, with findings identical to those of the ^{18}F-FDG PET/CT scan alone (no lesions missed). The results of this analysis are also detailed in Table 1. There was no disagreement (in this limited number of scans)

TABLE 1. Data from 14 Patients Included in Pilot Study and Results of PET/CT Scans

Age (y)	Cancer	^{18}F-FDG findings	^{18}F findings	Cocktail findings	Cocktail vs. ^{18}F	Cocktail vs. ^{18}F-FDG
75	Prostate	Ribs, pelvis, femur, LNs	Skull, ribs, T/L, pelvis, femur	Skull, ribs, T/L, pelvis, femur, LNs	Equal	Equal
59	Lung	LUL nodule, LN	Negative	LUL nodule, LN	Equal	Equal
65	Prostate	Pelvic LNs	Negative	Pelvic LNs	Equal	Equal
68	Colon	Liver, scapula, C/T/L, pelvis	Skull, scapula, ribs, C/T/L, pelvis, femurs	Liver, skull, scapula, ribs, C/T/L, pelvis, femurs	Equal	Equal
31	Sarcoma	Right thigh, B/L lung nodules	Negative	Right thigh, B/L lung nodules	Equal	Equal
44	Sarcoma	Soft-tissue mass	Skull, T10, pubis	Soft-tissue mass, T10, pubis	Lesion missed in the skull on cocktail	Equal
41	Sarcoma	Right femur	Right femur	Right femur	Equal	Equal
70	Prostate	Negative	Scapula, ribs	Scapula, ribs	Equal	Equal
55	Breast	Negative	Negative	Negative	Equal	Equal
55	Breast	Liver	Negative	Liver	Equal	Equal
19	Sarcoma	Rib, soft-tissue mass	Rib	Rib	Equal	Equal
63	Sarcoma	Negative	Negative	Negative	Equal	Equal
30	Sarcoma	Left gluteus	Negative	Left gluteus	Equal	Equal
30	Paraganglioma	Soft-tissue mass, skull, scapula, ribs, C/T/L, humerus, pelvis, femurs	Skull, scapula, ribs, C/T/L, humerus, pelvis, femurs	Soft-tissue mass, skull, scapula, ribs, C/T/L, humerus, pelvis, femurs	Equal	Equal

LNs = lymph nodes; T/L = thoracic and lumbar spine; LUL = left upper lung; C/T/L = cervical, thoracic, and lumbar spine; B/L = bilateral.

between the readers. In Figure 4, we present images of a 75-y-old man with prostate cancer (patient 1).

Evaluation of ^{18}F PET/CT Versus ^{18}F-FDG PET/CT in Humans

In 6 patients, the skeletal disease was more extensive on the ^{18}F PET/CT scan than on the ^{18}F-FDG PET/CT scan, whereas in another patient ^{18}F PET/CT showed osseous metastases and ^{18}F-FDG PET/CT findings were negative. The remaining 7 patients had no osseous metastases identified on the ^{18}F PET/CT or the ^{18}F-FDG PET/CT scans.

DISCUSSION

The spatial resolution of ^{99m}Tc-MDP skeletal scintigraphy and SPECT affects their sensitivity for detecting osseous metastases. Thus, the transition to the better resolution of PET/CT for detection of osseous metastases appears appealing, with the positron emitter ^{18}F as the radiotracer of choice. ^{18}F PET/CT was proved to be superior in bone lesion detection over a ^{99m}Tc-MDP bone scan and SPECT (*6*).

^{18}F-FDG PET/CT contributes unique information about the metabolic activity of musculoskeletal lesions (*7*). However, several researchers concluded that ^{99m}Tc SPECT is superior to ^{18}F-FDG PET in detecting bone metastases in breast cancer, and the sensitivity for osteoblastic lesions is limited with ^{18}F-FDG PET/CT (*8,9*). For prostate cancer, evidence exists that ^{18}F-FDG PET is less sensitive than bone scintigraphy. ^{18}F-FDG PET is limited in the detection of osseous metastatic lesions but may be useful in the detection of metastatic nodal and soft-tissue disease (*10*). There is limited data relating to lymphoma, but the ^{18}F-FDG PET scan seems to perform better than does the bone scan. An increasing body of evidence relates to the valuable role of an ^{18}F-FDG PET scan in multiple myeloma, in which it is clearly better than the bone scan, presumably because ^{18}F-FDG is identifying marrow-based disease at an early stage (*11*). The precise localization of a metastasis in the skeleton may be important with regard to the extent of the metabolic response induced (*12*). ^{18}F-FDG PET may also have an important role in the imaging evaluation of patients with bone and soft-tissue sarcoma, including guiding biopsy, detecting local recurrence in amputation stumps, detecting metastatic disease, predicting and monitoring response to therapy, and assessing for prognosis (*13*).

The arguments mentioned here advocate for the use of both ^{18}F PET/CT and ^{18}F-FDG PET/CT for the initial staging of patients with cancer. In this prospective pilot study, we combined 2 scans in a single imaging procedure. To date, no clinical attempts to combine ^{18}F and ^{18}F-FDG administration in a single PET/CT examination have been reported. Hoegerle et al. reported the use of combined ^{18}F and ^{18}F-FDG administration for PET more than a decade ago, when PET/CT was not available (*14*). In their study, the images obtained after combined administration were not compared with separate ^{18}F and ^{18}F-FDG images obtained from each patient. Also, Hoegerle et al. attempted to use the skeletal ^{18}F uptake as a surrogate for anatomic localization of abnormal ^{18}F-FDG in the absence of fused PET and CT. With the availability of PET/CT, a cocktail approach allows for a new strategy for patient management not previously possible.

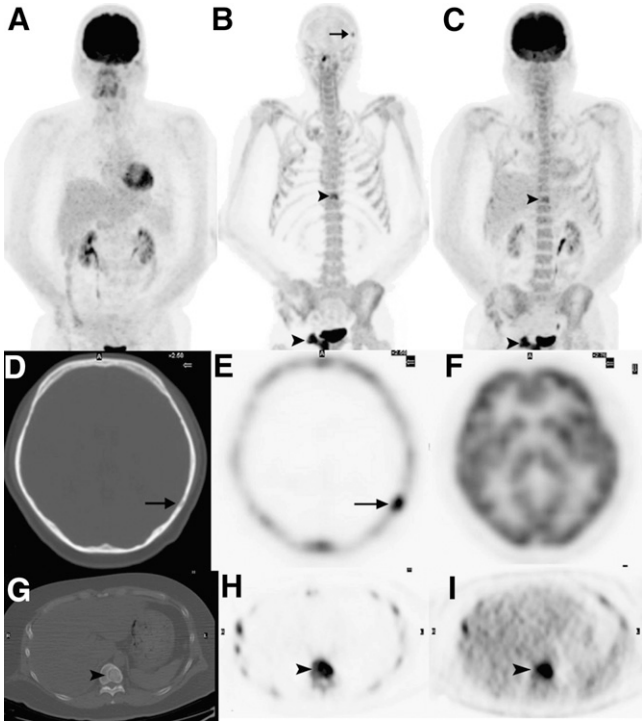

FIGURE 2. A 44-y-old man with soft-tissue sarcoma. (A) MIP image of ^{18}F-FDG PET shows normal radiotracer uptake. (B) MIP image of ^{18}F PET shows intense radiotracer uptake in skull lesion (arrow) and in T10 vertebra and right pubis (arrowheads). (C) Skull lesion is missed on MIP image of combined ^{18}F/^{18}F-FDG PET, but MIP image of combined ^{18}F/^{18}F-FDG PET shows skeletal lesions in T10 vertebra and right pubis noted on ^{18}F PET (arrowheads). Skull lesion (arrow) is seen on transaxial CT (D) and ^{18}F PET (E) but not on combined ^{18}F/^{18}F-FDG PET (F). Lesion in T10 vertebra (arrowhead) is seen on transaxial CT (G), ^{18}F PET (H), and combined ^{18}F/^{18}F-FDG PET (I).

We successfully separated the metabolic skeletal uptake and allowed interpretation of the ^{18}F and ^{18}F-FDG tissue distribution, even though the 2 tracers were administered at the same time. This approach is based on the eventual biodistribution of the ^{18}F nearly exclusively to the skeletal structures. We also showed that visual analysis of the combined cocktail ^{18}F/^{18}F-FDG PET/CT scan results in reliable diagnosis, compared with interpretation of the separate ^{18}F PET/CT and ^{18}F-FDG PET/CT scans.

In terms of radiation exposure for the patients, a ^{99m}Tc-MDP bone scan exposes patients to approximately 4.2 mSv (420 mrem) of radiation, and an ^{18}F-FDG PET/CT scan exposes them to approximately 26.5 mSv (2,650 mrem) (0.03 mSv/MBq [110 mrem/mCi]) from ^{18}F-FDG and 10 mSv [1,000 mrem] from the low-dose CT). This equals a total of 30.7 mSv (3,070 mrem) for the bone scan and ^{18}F-FDG scan together. The combination of ^{18}F PET/CT and ^{18}F-FDG PET/CT in a single examination will result in a total of 31.5 mSv (3,150 mrem) (0.03 mSv/MBq [110 mrem/mCi] from ^{18}F-FDG, 0.03 mSv/MBq [100 mrem/mCi] from ^{18}F, and 10 mSv [1,000 mrem] from the low-dose CT). The newest PET/CT

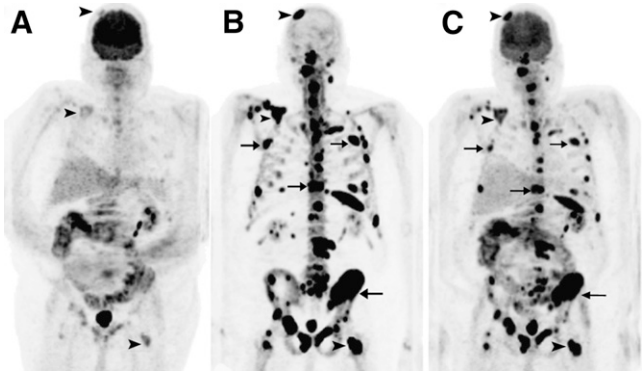

FIGURE 3. A 68-y-old man with colon cancer. (A) MIP image of ^{18}F-FDG PET shows faint radiotracer uptake in several skeletal lesions (arrowheads). (B) MIP image of ^{18}F PET shows intense radiotracer uptake in multiple bone lesions, including better visualization of lesions seen on ^{18}F-FDG PET (arrowheads) and more extensive skeletal metastases (arrows). (C) MIP image of combined ^{18}F/^{18}F-FDG PET shows skeletal lesions noted on ^{18}F PET (arrowheads).

scanners have increased sensitivity, and the dose of ^{18}F-FDG can be decreased to 370 MBq (10 mCi), resulting in a total radiation exposure of 26 mSv (2,600 mrem) from the combined ^{18}F/^{18}F-FDG PET/CT scan. Thus, instead of patients having to get separate SPECT and PET/CT studies, usually on different days, this strategy allows for 1 combined PET/CT study with potentially more utility, lower costs, lower radiation dose, and much greater patient convenience.

One limitation of our study is the small number of patients included in this pilot phase and the selection bias toward patients with known cancers. To come to statistically sound conclusions regarding the appropriate indications for the combined ^{18}F/^{18}F-FDG PET/CT study, further prospective enrollment of patients is needed. Also, analysis

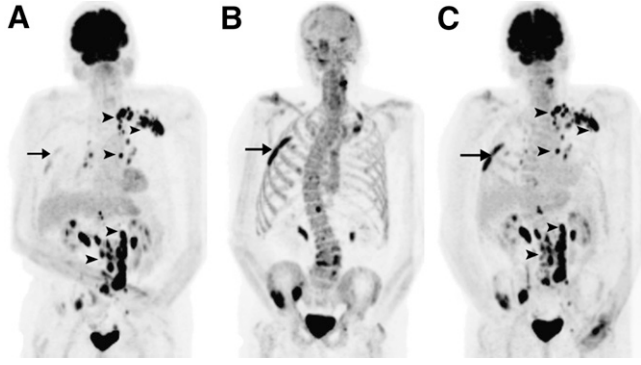

FIGURE 4. A 75-y-old man with prostate cancer. (A) MIP image of ^{18}F-FDG PET shows lymph node metastases (arrowheads) and faint uptake in osseous lesions, such as a right rib (arrow). (B) MIP image of ^{18}F PET shows intense radiotracer uptake in multiple bone lesions, including right rib lesion (arrow) seen on ^{18}F-FDG PET. (C) MIP image of combined ^{18}F/^{18}F-FDG PET shows both lesions noted on ^{18}F-FDG PET (arrowheads) and skeletal lesions noted on ^{18}F PET (reference right rib lesion marked with arrow).

of the 3 different PET/CT scans might not be fully independent because of the short interval between interpretation of the 3 scans of the same patient. In addition, none of the 14 patients received therapy with bone marrow–stimulating agents before imaging. Bone marrow–stimulating therapy induces intense ^{18}F-FDG uptake in the skeleton (*15*) and may play a confounding role in the evaluation of the osseous structures on the combined ^{18}F/^{18}F-FDG scan. This particular instance of evaluation of response to therapy by combined ^{18}F/^{18}F-FDG PET/CT needs to be separately evaluated in future studies. The bone-mask technique has the limitation of possible inclusion of the soft-tissue component of a lesion that is contiguous with the bone surface. Thus, it is possible that soft-tissue lesions can be captured and displayed as skeletal disease. Further iterations of the software used, with careful analysis of edge detection, are warranted to address this issue.

CONCLUSION

Our pilot-phase prospective trial demonstrated the feasibility of combined administration of ^{18}F/^{18}F-FDG in a single PET/CT examination for detection of malignancy. The use of a single examination opens the possibility for improved patient care. Both visual analysis of the combined ^{18}F/^{18}F-FDG PET/CT scan and interpretation of the processed images were accurate in this selected population with known cancers, who had been referred for determination of the extent of disease before therapy. Larger prospective trials are needed for a better understanding of the precise indications for the combined ^{18}F/^{18}F-FDG PET/CT method and for refinement of the image-processing algorithm.

ACKNOWLEDGMENTS

We thank Dr. Fred Chin in the Cyclotron Facility, Lindee Burton, and all the technologists in the Nuclear Medicine Clinic. This research was supported in part by NCI ICMIC CA114747 (SSG), and the clinical studies were supported in part by the Doris Duke Foundation and Canary Foundation.

REFERENCES

1. Gambhir SS. Molecular imaging of cancer with positron emission tomography. *Nat Rev Cancer.* 2002;2:683–693.
2. Kapoor V, McCook BM, Torok FS. An introduction to PET-CT imaging. *Radiographics.* 2004;24:523–543.
3. Podoloff DA, Advani RH, Allred C, et al. NCCN task force report: positron emission tomography (PET)/computed tomography (CT) scanning in cancer. *J Natl Compr Canc Netw.* 2007;5(suppl 1):S1–S22.
4. Savelli G, Maffioli L, Maccauro M, De Deckere E, Bombardieri E. Bone scintigraphy and the added value of SPECT (single photon emission tomography) in detecting skeletal lesions. *Q J Nucl Med.* 2001;45:27–37.
5. Shirazi PH, Rayudu GV, Fordham EW. ^{18}F bone scanning: review of indications and results of 1,500 scans. *Radiology.* 1974;112:361–368.
6. Even-Sapir E, Metser U, Mishani E, Lievshitz G, Lerman H, Leibovitch I. The detection of bone metastases in patients with high-risk prostate cancer: ^{99m}Tc-MDP planar bone scintigraphy, single- and multi-field-of-view SPECT, ^{18}F-fluoride PET, and ^{18}F-fluoride PET/CT. *J Nucl Med.* 2006;47:287–297.
7. Feldman F, van Heertum R, Manos C. ^{18}FDG PET scanning of benign and malignant musculoskeletal lesions. *Skeletal Radiol.* 2003;32:201–208.
8. Uematsu T, Yuen S, Yukisawa S, et al. Comparison of FDG PET and SPECT for detection of bone metastases in breast cancer. *AJR.* 2005;184:1266–1273.
9. Nakai T, Okuyama C, Kubota T, et al. Pitfalls of FDG-PET for the diagnosis of osteoblastic bone metastases in patients with breast cancer. *Eur J Nucl Med Mol Imaging.* 2005;32:1253–1258.
10. Jadvar H, Pinski JK, Conti PS. FDG PET in suspected recurrent and metastatic prostate cancer. *Oncol Rep.* 2003;10:1485–1488.
11. Jadvar H, Conti PS. Diagnostic utility of FDG PET in multiple myeloma. *Skeletal Radiol.* 2002;31:690–694.
12. Fogelman I, Cook G, Israel O, Van der Wall H. Positron emission tomography and bone metastases. *Semin Nucl Med.* 2005;35:135–142.
13. Jadvar H, Gamie S, Ramanna L, Conti PS. Musculoskeletal system. *Semin Nucl Med.* 2004;34:254–261.
14. Hoegerle S, Juengling F, Otte A, Altehoefer C, Moser EA, Nitzsche EU. Combined FDG and [F-18]fluoride whole-body PET: a feasible two-in-one approach to cancer imaging? *Radiology.* 1998;209:253–258.
15. Kazama T, Swanston N, Podoloff DA, Macapinlac HA. Effect of colony-stimulating factor and conventional- or high-dose chemotherapy on FDG uptake in bone marrow. *Eur J Nucl Med Mol Imaging.* 2005;32:1406–1411.